JOURNAL OF FUEL CHEMISTRY AND TECHNOLOGY
Volume 54, Issue 3, March 2026

燃料化学学报(中英文)
Journal of Fuel Chemistry and Technology

Cite this article as: J Fuel Chem Technol, 2026, 54, 20250187

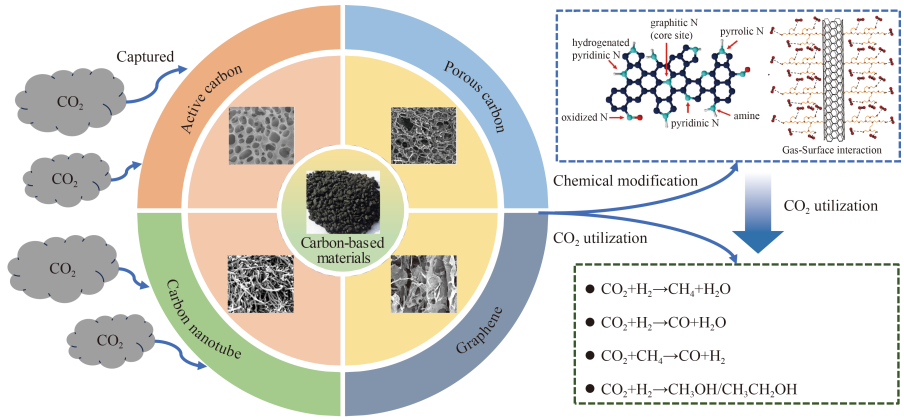
REVIEW

Recent advances in carbon-based materials for CO_2 capture and utilization

FU Lang[1], YAO Dingding[1,*], HU Qiang[2], YAN Shuiping[1], YANG Haiping[2]

[1] College of Engineering, Huazhong Agricultural University, Wuhan 430070, China;
[2] State Key Laboratory of Coal Combustion, Huazhong University of Science and Technology, Wuhan 430074, China

Abstract: CO_2 capture and utilization (CCU) technologies have been recognized as crucial strategies for mitigating global warming, reducing carbon emission, and promoting resource circularity. As such, the design and development of related materials have attracted considerable research attention. Carbon-based materials, characterized by tunable pore structures, abundant active sites, high specific surface area, and excellent chemical stability, demonstrate significant potential for applications in CO_2 capture and utilization. This review systematically analyzes the adsorption behaviors and performance variations of typical carbon materials, including activated carbon, porous carbon, graphene, and carbon nanotubes during CO_2 capture processes. Concerning CO_2 utilization, emphasis is placed on recent advances in the catalytic applications of carbon-based materials in key reactions such as methanation, reverse water-gas shift, dry reforming of methane, and alcohol synthesis. Moreover, the benefits and drawbacks of carbon materials in terms of CO_2 adsorption capacity, catalytic activity, and stability are thoroughly evaluated, and their potential applications in integrated CO_2 capture and utilization technologies are discussed. Finally, key strategies for enhancing the performance of carbonaceous materials through structural modulation and surface modification are elucidated. This review aims to provide theoretical guidance for the future development and large-scale implementation of carbon-based materials in CCU technologies.



Key words: CO_2 capture and utilization; carbon materials; adsorption; catalysis

Global warming is strongly correlated with greenhouse gas emissions. Rising temperatures have led to sea level rise, polar ice melt and frequent extreme weather events, threatening human survival and severely undermining prospects for achieving sustainable development[1]. As a primary greenhouse gas (accounting for approximately 25% of global warming), CO_2 predominantly originates from fossil fuel combustion. In such context, developing carbon capture and utilization (CCU) technology has emerged as a critical pathway toward global carbon neutrality. CCU technology converts CO_2 into high-value products, such as methane and alcohols *via* CO_2 hydrogenation, isomeric alkanes, or syngas (H_2/CO) through dry reforming with CH_4, reducing reliance on fossil fuels while enabling CO_2 resource utilization[2]. Via chemical modification or physical engineering techniques, the pore architecture and surface functional groups of carbon-based materials can be precisely tailored to optimize catalytic performance. Meanwhile, the nanoscale dispersion characteristics of carbon materials enhance the utilization efficiency of

Received: 2025-07-31; Revised: 2025-08-19
Foundation items: Supported by National Key R&D Program of China (2025YFE0109700), and the National Natural Science Foundation of China (52106150).
* Corresponding author. E-mail: dingdingyao@mail.hzau.edu.cn.
DOI: 10.1016/S1872-5813(25)60604-9 CSTR: 32157.14.2097-213X.2025.JFCT.0148
本文的英文电子版由 Elsevier 出版社在 ScienceDirect 上出版 (http://www.sciencedirect.com/science/journal/18725813)

catalytic active sites, broadening their prospects for CO_2 conversion applications[3].

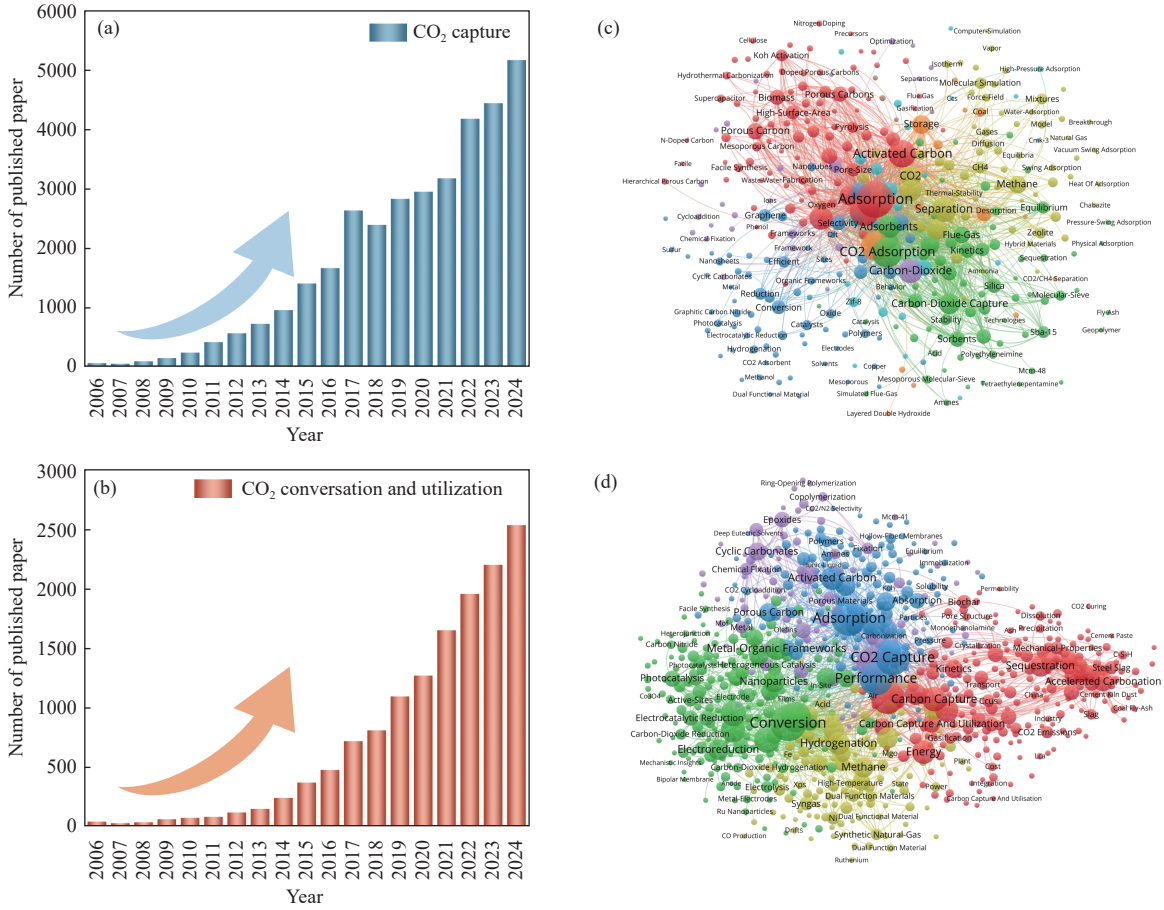
The number of scientific papers on carbon-based materials in the CCU field has increased significantly in recent years, both domestically and internationally, as shown in Figure 1. Regarding the application of carbon-based materials for CO_2 capture, existing reviews have stated biochars, porous carbons, or activated carbons (AC) for CO_2 capture, typically focusing on activation mechanisms[4–6]. However, reviews on the application of carbon materials in the field of CO_2 capture and utilization remain limited. Therefore, this paper provides a systematic summary of the current applications of widely used carbon-based materials in CO_2 capture and utilization. Key aspects include, elucidating CO_2 adsorption and catalytic mechanisms, comparing the performance of carbon-based materials and metal oxide-based materials, and exploring the potential applications of carbon materials in integrated carbon capture and utilization (ICCU) technology. Finally, limitations of carbonaceous adsorbents and carbon-supported catalysts are identified, with targeted strategies proposed to address these challenges.

1 Carbon materials in CO_2 capture

According to the dimensional classification, carbon-based materials can be categorized into 0D, 1D, 2D, 3D materials. By modifying carbon-based materials of various dimensional with tailored surface functional groups, their functionality can be tuned to enable diverse CO_2 capture and conversion reactions[7].

1.1 Porous carbon for CO_2 capture

The 3D carbonaceous adsorbents is characterized by highly developed pore structures and large specific surface area. It can be prepared through processes such as carbonization, activation, and templating methods, and its raw materials are widely available[8]. Converting biomass waste into high-performance CO_2 adsorbents has garnered significant attention due to the carbon neutrality of the feedstock.



(a), (c): Carbon materials applied to CO_2 adsorption, keywords for "carbon materials" and "CO_2 adsorption";
(b), (d): carbon materials applied to CO_2 utilization, keywords for "carbon materials" and "CO_2 utilization".

Fig. 1 Network visualization showing the publication count and keywords in related studies from 23 June, 2006 to 23 June 2024 (date source: Web of Science)

Wu et al.[9] reported nitrogen and sulfur co-doped porous carbon adsorbents synthesized from discarded bamboo shoot shells as the carbon source, thiourea as a nitrogen and sulfur co-doping agent, and potassium carbonate as the activator. Under conditions of 0 °C and 1 bar, this material displayed excellent CO_2 adsorption capacity with the maximum of 5.93 mmol/g. Gorbounov et al.[10] prepared porous carbon from biomass combustion bottom ash using KOH activation. The material exhibited a specific surface area of 643.6 m^2/g. At 1 bar, its CO_2 adsorption capacity was 1.93 mmol/g at 25 ℃ and 1.29 mmol/g at 50 ℃. Notably, these adsorption capacities were four times higher than those of unactivated porous carbon and twice those of physically activated porous carbon. To be noted, the material also demonstrated excellent cyclic stability, maintaining 85% of its initial adsorption capacity after 40 adsorption-desorption cycles.

Characterized by high activation levels and developed pore structures, both activated carbon and porous carbon possess high specific surface areas and hierarchical pore architectures; however, their pore structures exhibit distinct differences. Activated carbon is characterized by a high proportion of micropores and larger specific surface area, while porous carbon is typically dominated by mesopores and macropores and contains fewer micropores[11]. Yang et al.[12] prepared an amine-modified biochar from coconut shells by impregnating with diethylenetriamine (DETA), triethylenetetramine (TETA), and tetraethylenepentamine (TEPA). The results revealed that these amine groups increased the number of CO_2 adsorption active sites, effectively enhancing the CO_2 adsorption performance of the activated carbon. Weldekidan et al.[13] employed citrus peels as precursors, preparing porous activated carbon through KOH chemical activation and a two-step KOH-alumina chemical activation process. The specific surface areas of the resulting materials were 1113 and 2143 m^2/g, respectively; the KOH-activated carbon materials outperformed with the CO_2 uptake of 4.56 mmol/g (at 0 °C and 1 bar). Phadungbut et al.[14] utilized waste wooden chopsticks as the raw material with $ZnCl_2$ and KOH as activating agents, respectively. The results showed KOH-activated materials achieved superior CO_2 adsorption capacity (115.7 mg/g). Activated carbon was synthesized from olive kernels using banana peel extract as activating agent. The material displayed a specific surface area of 915 m^2/g and a pore volume of 0.495 cm^3/g, and its CO_2 adsorption capacities reached to 6.32 mmol/g at 0 °C and 4.33 mmol/g at 30 °C, with excellent cyclic stability maintained after 50 cycles[15]. These studies collectively demonstrate that alkali modification offers distinct advantages in enhancing the CO_2 capture performance of activated carbon. Alkalinity is recognized as the determinant factor governing CO_2 adsorption performance. As an acidic gas, CO_2 undergoes acid-base reactions with strongly basic functional groups introduced onto the material surface, such as nitrogen-containing groups or alkaline metal oxides, which donate lone pairs of electrons to promote chemical adsorption of CO_2, thereby substantially elevating the adsorption capabilities of materials[16].

According to the above analysis, whether the materials are highly microporous activated carbons or other porous carbons dominated by mesopores and macropores, their precursors are extensively available, and can be valorized *via* pyrolysis (Figure 2).

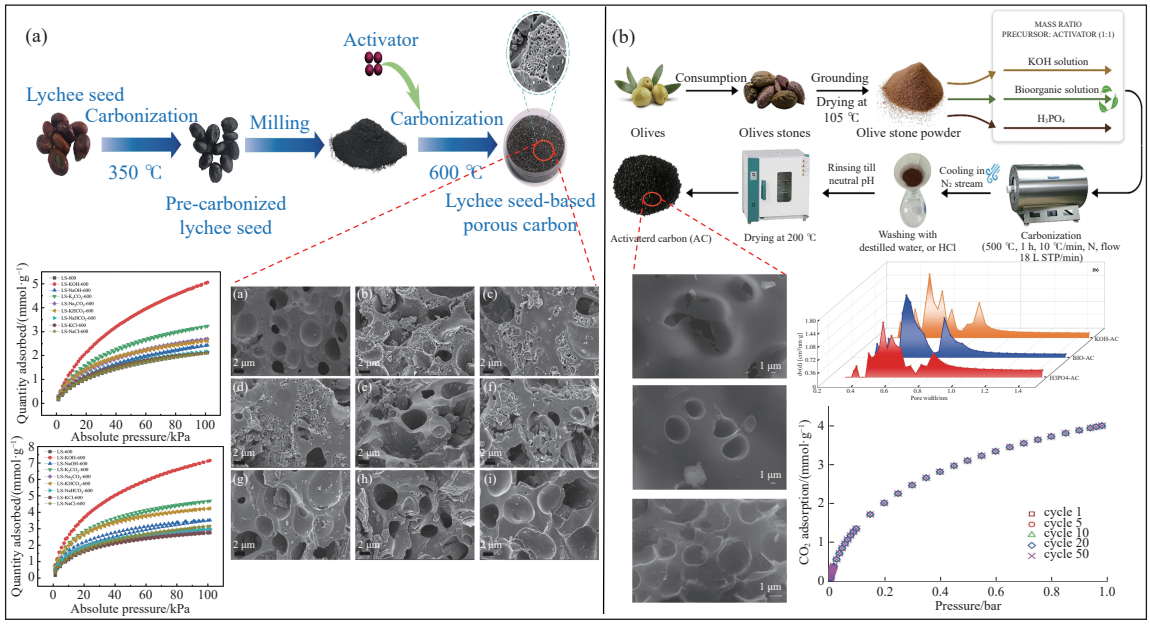


Fig. 2 Structural characteristics and CO_2 adsorption performance of carbon materials prepared by pyrolysis of different biomasses ((a) porous carbon prepared by pyrolysis of lychee seeds, (b) activated carbon prepared by pyrolysis of olive pits[15,17]) (with permission from Elsevier)

These materials are generally endowed with favorable CO_2 adsorption properties, ensuring promising prospects for industrial applications while aligning with fundamental principles of sustainable development.

1.2 Graphene for CO_2 capture

Graphene and its derivatives encompass multiple types. Based on the number of layers, they can be classified into single-layer, few-layer, and multi-layer graphene; derivatives primarily include graphene oxide (GO), graphene nanosheets, and reduced graphene oxide (RGO)[1].

To enhance the CO_2 adsorption performance, Kumar et al.[18] reported a strategy of synthesizing GO adsorbents by involving oxalic acid reduction combined with ultraviolet activation. The resultant material yields a specific surface area of 577.3 m^2/g. At 25 °C, the CO_2 adsorption capacity reached 1.65 mmol/g, while at 100 °C, the CO_2 recovery rate achieved 98.8%, which was markedly higher than that of non-ultraviolet-activated samples (88.4%), and exhibited rapid desorption kinetics and excellent cyclic stability. Roble et al.[19] investigated the mechanisms by which heteroatom doping and film architecture modulate the CO_2 adsorption behavior of GO and its derivatives. The findings revealed that both nitrogen doping and sulfur modification enhanced the CO_2 adsorption capacity of materials by introducing Lewis basic sites and increasing porosity respectively. Additionally, CO_2 adsorption equilibrium time was significantly prolonged by thicker film architectures, and internal diffusion rate became the critical factor governing adsorption kinetics. Safaei et al.[20] synthesized GO *via* an improved Hummers method (utilizing H_2SO_4, $KMnO_4$ and H_2O_2) and subsequently fabricated three-dimensional graphene aerogels through hydrothermal treatment coupled with freeze-drying techniques. The resulting aerogel had a micropore surface area that constituted 33% of the total micropore plus mesopore surface area. During GO synthesis, the high-dose H_2SO_4 successfully constructed abundant macroporous structures, achieving a CO_2 adsorption capacity of 1.72 mmol/g. Current research on graphene applications for CO_2 capture is predominantly focused on single modification approaches; multi-method collaborative optimization could be explored in future studies. For instance, combining nitrogen doping with pore structure engineering could simultaneously enhance molecular interactions *via* nitrogen sites while improving mass transfer efficiency through hierarchical pore architecture, thereby further increasing adsorption capacity.

1.3 Carbon nanotubes for CO_2 capture

Carbon nanotubes (CNTs), typically derived from graphite, primarily encompass single-walled carbon nanotubes and multi-walled carbon nanotubes (MWCNTs). Their hollow architectures and high aspect ratios create favorable conditions for CO_2 adsorption by providing abundant pores and large specific surface areas. Furthermore, CNTs can be functionalized to meet specific adsorption requirements[21]. Whether used to modify other metal oxides to enhance CO_2 adsorption or serving as standalone adsorbents, CNTs demonstrate versatile applicability.

As modifiers, CNTs were incorporated into CaO in the study conducted by Oliveira et al.[22], revealing that merely 0.05% CNT addition significantly enhanced the porosity of the adsorbent, thereby increasing its CO_2 capture efficiency from 64.1% to 98.2% and adsorption capacity from 11.43 to 17.52 mmol/g. Heidari et al.[23] fabricated $CaZrO_3$-CaO adsorbents doped with different amount of CNT. It was observed that the hybrid material doped with 5% CNTs exhibited optimal performance, with its CO_2 capture capacity even improving after 15 adsorption-desorption cycles. As standalone adsorbents, Irani et al.[24] immobilized tetraethylenepentamine (TEPA) onto KOH-modified CNTs. At 75% TEPA loading, the material achieved the highest CO_2 adsorption capacity of 5 mmol/g under simulated flue gas conditions containing 10% CO_2 and 1% H_2O. Similarly, Lee et al.[25] prepared polyethyleneimine (PEI)-impregnated MWCNTs (MWCNTs/PEI) *via* wet impregnation, as illustrated in Figure 3. The relevant thermogravimetric analysis revealed that the CO_2 adsorption capacity of MWCNTs/PEI was significantly higher than that of unmodified MWCNTs. This enhancement was primarily attributed to the attachment of amine groups onto the MWCNT surface during impregnation, which created additional CO_2 adsorption sites. The acid-base interactions between amine groups and CO_2 molecules effectively strengthened the adsorption performance.

CNTs demonstrate potential in flue gas carbon capture due to their highly efficient adsorption performance in low-concentration CO_2 atmospheres, particularly for integration with existing combustion systems. Nevertheless, significant challenges remain, in particular surface-modified functional groups may undergo thermal decomposition when exposed to high temperature common in industrial waste-heat environment. Future research could prioritize breakthroughs in technologies designed to improve the thermal stability of surface-modified functional groups.

1.4 Comparison of CO_2 capture performance between carbon-based and metal oxide-based materials

Notwithstanding both carbon-based materials and metal oxide-based materials exhibit excellent potentials in CO_2 capture performance, they diverge significantly in adsorption mechanisms, practical capacities, and cyclic stability. Table 1 lists the CO_2 adsorption performance of various carbon-based materials and metal oxide-based materials under different conditions. Carbon-based materials predominantly rely on physical adsorption, yet chemical adsorption can be achieved through surface functional group modification[15]. Their advantages lie in the capability to achieve efficient CO_2 capture at low temperatures *via* pore structure regulation and heteroatom doping.

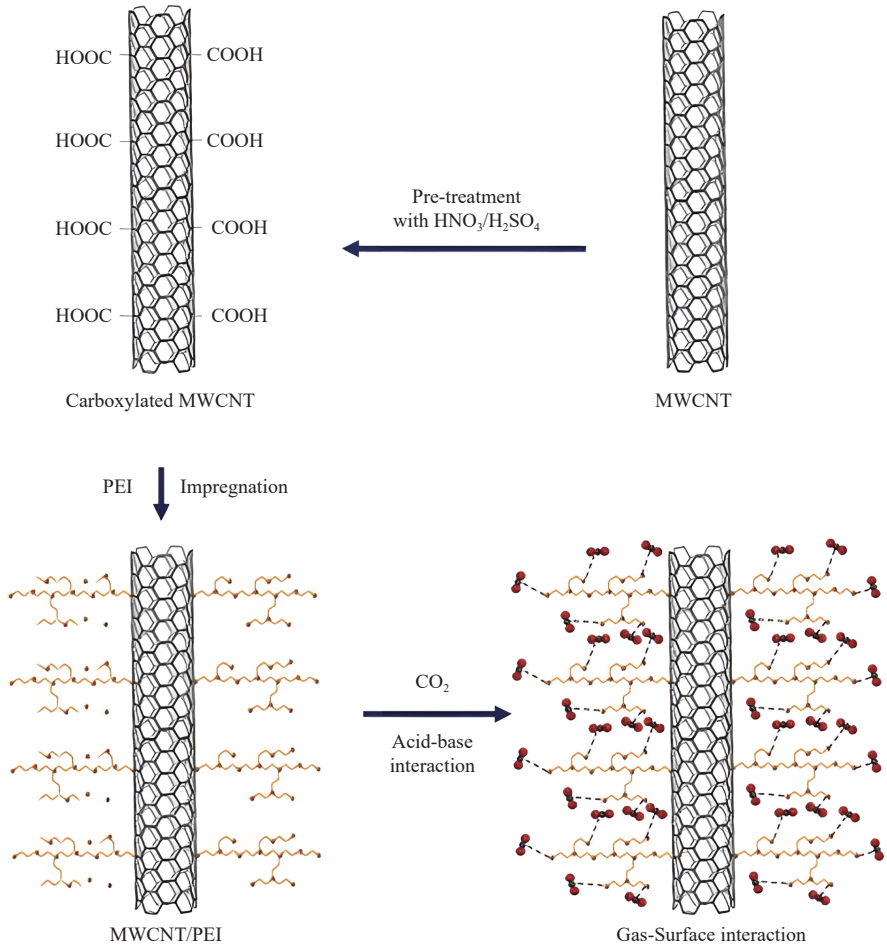


Fig. 3 Schematic diagram of the CO_2 adsorption mechanism of PEI-impregnated MWCNTs[25] (with permission from Elsevier)

In contrast, metal oxides undergo chemical adsorption, wherein CO_2 is immobilized on the adsorbent surface in the form of carbonates. Although metal oxides typically possess higher theoretical CO_2 adsorption capacities, practical applications are frequently hindered by the formation of carbonate product layers, which readily induce pore blocking and lead to significant reductions in adsorption capacity[26]. Regarding cyclic stability, carbon-based materials, predominantly governed by physical adsorption, require milder regeneration conditions and consequently exhibit superior cycling stability compared to most metal oxides. Additionally, they can be applied in complex flue gas environments due to their excellent chemical stability. In contrast, the regeneration processes of metal oxides demand high-temperature treatments, which readily result in severe sintering and deactivation phenomena. In addition, acidic gases present in flue gas can also deteriorate their structures.

2 Carbon materials in CO_2 utilization

Propelled by the rapid advancement of renewable energy sources, key technologies for green hydrogen production are experiencing accelerated development, with technological breakthroughs and declining cost laying the foundation for their large-scale deployment. In this context, hydrogenation of carbon dioxide for the synthesis of fuels and chemicals simultaneously addresses challenges in wind-solar power consumption and CO_2 valorization, facilitating efficient CO_2 conversion and recycling[27]. In the following sections, research progress concerning the application of various carbon materials in catalyzing CO_2 conversion into diverse products is systematically reviewed.

2.1 Carbon materials for CO_2 methanation reaction

From a thermodynamic perspective, CO_2 methanation display distinct advantages, wherein hydrogen atoms progressively replace oxygen atoms from CO_2 molecules to ultimately form CH_4. Compared to other CO_2 conversion routes, methanation reactions not only exhibit higher reactivity but also require relatively mild reaction conditions[27].

Regarding to pure carbon materials, the relevant research for catalyzing methanation reactions remains limited. Instead, catalytic conversion of CO_2 to methane is typically achieved by loading active metal catalysts onto carbon supports. The Ni/AC catalyst prepared by Cam et al.[28] achieved a 76% CO_2 conversion rate at 400 °C.

Table 1 Summary of adsorption performance of carbon materials and metal oxides

Materials	Adsorbent	Precursor	Activation technique	BET surface area/($m^2 \cdot g^{-1}$)	Total pore volume /($cm^3 \cdot g^{-1}$)	Pressure (bar); Temperature /K	Adsorption capacity /($mmol \cdot g^{-1}$)	Ref.
Carbon-based	Porous carbons	Phenolic resins	Chemical (Melamine)	1013−1051	−	1; 273	2.68−4.32	[29]
	Porous carbons	Chinese fir bark	Chemical (KOH)	1384−1506	0.04−1.07	1; 273	4.00−7.00	[30]
	AC	Olive stones	Chemical (banana plant extract)	915	0.495	1; 273	6.32	[15]
	AC	Chitosan	Chemical (K_2CO_3)	1355.0	0.60	1; 298	4.69	[31]
	Monolithic graphene	Graphite powder	Physical (UV activated)	577.3	1.59	1; 298	1.65	[18]
	Three-dimensional graphene-based	Graphite powder	Chemical (H_2SO_4)	1315.98	1.07	1; 273	3.36	[32]
	CNTs	Multi walled carbon nanotubes	Chemical (TEPA)	−	−	1; 333	5	[24]
	Acicular hollow porous carbon/CNTs	Polydopamine	Chemical (Ca_2CO_3)	561	−	1; 273	4.43	[33]
Metal oxides	CaO/CuO	$Ca(NO_3)_2 \cdot 4H_2O$ $Cu(NO_3)_2 \cdot 3H_2O$	Chemical ($C_6H_{12}O_6$)	6.8−9.1	0.012−0.027	1; 923	3.18−5	[34]
	$Mn_yP_2D_{30}$-CaO	Calcium acetate $Mn(NO_3)_2$	Chemical (Citric acid)	6.22−10.71	0.022−0.080	1; 973	5.63−13.66	[35]
	CeCaO	$Ca(NO_3)_2 \cdot 4H_2O$ $Ni(NO_3)_2 \cdot 6H_2O$	Chemical (Citric acid)	−	−	1; 823	10.6−15.3	[36]
	MgO	MgO(98%)	Chemical (Alkali metal nitrate salt)	10.3−14.6	0.045−0.077	1; 473−553	1.97−5.56	[37]
	MgO	Mg(99.9%) $MgCO_3$(98%)	−	3.68−18.00	0.053−0.11	1; 573	0.31−0.37	[38]
	Al_2O_3	γ-Al_2O_3	Chemical (TEPA)	264.1−429.6	0.27−0.99	1; 323	2.04	[39]
	Nano-Al_2O_3	Coal fly ash	Chemical (PEI)	−	−	0.4; 363	3.05	[40]

Its superior catalytic activity is primarily attributed to the large specific surface area of activated carbon, which facilitates Ni particle dispersion and effectively inhibits deactivation caused by agglomeration. Additionally, the reducibility of the active metal is enhanced. While noble metal oxides such as ZrO_2 and CeO_2 exhibit high CO_2 conversion efficiency, their large-scale application is constrained by high costs[41]. To address this limitation, Quatorze et al.[42] developed composite catalysts by integrating ZrO_2 with activated carbon and CNTs, respectively. As illustrated in Figure 4, Ni/CNTs-ZrO_2 outperformed Ni/AC-ZrO_2 at lower temperatures (370 °C), achieving an 85.6% CO_2 conversion rate and 99.9% CH_4 selectivity. Surface modification of carbon materials can further enhance the catalytic performance of carbon-based catalysts in CO_2 methanation. Ni/AC catalysts prepared *via* reduction following O/N co-doping and thermal treatment exhibited significantly improved CO_2 adsorption capacity. This enhancement is attributed to π electron enrichment, which increases the number of Lewis basic active sites. Moreover, proton attraction promotes uniform Ni dispersion across the support surface, thereby demonstrating excellent catalytic performance (76% CO_2 conversion, 97% CH_4 selectivity)[43]. The aforementioned studies demonstrate that material design strategies, including elemental doping, composite support construction, and precise regulation of acid-base sites can effectively improve the catalytic performance of carbon-based catalysts in CO_2 methanation reactions.

Ni-loaded biochar (SCBB) was prepared by Gamal et al.[44] using pyrolyzed bagasse as the raw material. The biochar exhibited honeycomb-like and hexagonal pore structures, along with high specific surface area and porosity, which facilitated the full exposure of active sites, thereby enhancing catalytic efficiency. At 500 °C, a CO_2 conversion rate of 58% was achieved for 0.5Ni/SCBB. In another study[45], Ni and Ce-loaded activated biochar (Ni/Ce-ABC) catalysts were synthesized through an *in situ*

$NaHCO_3$ activation using pine wood as the precursor. Under conditions of 360 °C and 1 bar, these catalysts demonstrated CO_2 conversion and CH_4 selectivity of 88.6% and 92.3%, respectively. It was revealed that the excellent dispersion of Ce promoted the uniform distribution of Ni and simultaneously enhanced the CO_2 adsorption capacity of the biochar.

In the study conducted by Hu et al.[46], Ni-Ce/RGO catalysts modified with CeO_2 achieved an 84.5% CO_2 conversion rate and 83.0% CH_4 yield. Their exceptional catalytic performance primarily stems from oxygen vacancies in CeO_2, which enhance methanation reaction kinetics. Meanwhile, the oxygen-rich functional groups in RGO and its high surface area facilitate stable anchoring and dispersion of active metals. Additionally, RGO's rapid electron migration significantly boosts catalytic activity[47]. Additionally, Ma et al.[48] embedded graphene into nickel foam substrates to construct Ni-SiO_2/GO-Ni-foam catalysts, establishing strong metal-support interactions. These catalysts exhibit efficient and stable CO_2 methanation at high temperatures due to their high hydroxyl content and well-dispersed nickel species. Density functional theory (DFT) calculations reveal the critical role of graphene: it reduces dissociation energy barriers for H_2 and CO_2 while modifying SiO_2 electronic structure. As the consequence, the related CO_2 adsorption energy and Ni_4 cluster binding energy are enhanced.

Ma et al.[49] developed a CNTs-Al_2O_3 (CAS) composite carrier featuring abundant mesoporous structures and hydrophobicity. When loaded with catalysts, it achieved 49.62% CO_2 conversion and 95.98% CH_4 selectivity at 250 °C and 1.5 MPa, significantly outperforming catalysts using pure CNTs or Al_2O_3 supports. Compared to monolithic CNTs, the unique pore structure in CAS carrier imposed a confinement effect that remarkably prolonged the residence time of CO_2 molecules and reaction intermediates near active sites, thus leading to higher CO_2 conversion. In another study[50], N-doped CNT-supported Ni (Ni/CNTs-N) catalysts demonstrated 81.2% CO_2 conversion and 99.2% CH_4 selectivity at 400 °C while maintaining stability over 48 h under continuous operation. Mechanistic analysis revealed that N atoms provided additional anchoring sites for Ni, significantly improving Ni dispersion and metal-support interaction strength. This enhancement further augmented H_2 adsorption capacity, a key factor that critically influenced the overall catalytical performance. The composite carrier design thereby opened new pathways for functionalizing CNTs. Mhadmhan et al.[51] fabricated nickel-based CNTs-silica fiber (Ni/CNTs-SF) catalysts exhibiting superior adsorptive and catalytic performance compared to pure SiO_2 porous or fiber supports. This enhancement originated from the composite's high accessibility to reactants, its smaller Ni crystallite sizes, and a consequent strengthening of metal-support interaction. Collectively, these factors enhanced active metal dispersion and CO_2 methanation efficiency.

The microstructure of carbon materials, specifically their specific surface area, pore distribution, and surface chemistry, constitutes the pivotal factors in catalytic performance. For example, the tubular structure of CNTs stabilizes metal nanoparticles against migration and sintering, while the two-dimensional layered structure of graphene facilitates charge transfer acceleration, thereby enhancing reaction kinetics. Furthermore, by regulating CNT tube diameters and defect density in graphene, the metal-support interaction can be further optimized to achieve superior catalytic performance.

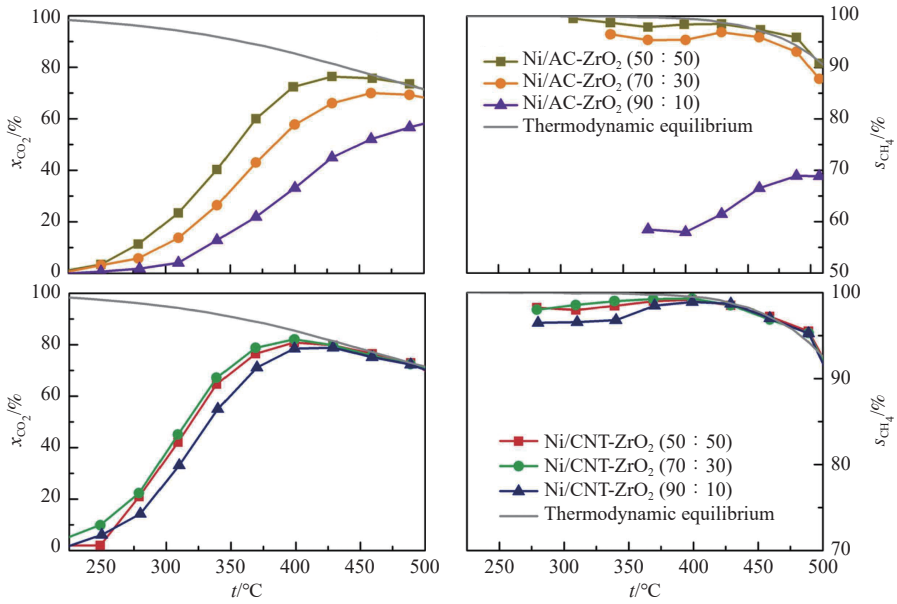


Fig. 4 Comparison of catalytic performance of Ni-loaded composites with different carbon-to-ZrO_2 ratios at different temperatures[42]
(with permission from Elsevier)

2.2 Carbon materials for reverse water-gas shift reaction

The reverse water-gas shift (RWGS) reaction typically proceeds at elevated temperatures exceeding 650 °C. However, such high temperatures readily induce catalyst sintering or coking, which reduces the number of active sites and consequently diminishes CO production efficiency[52]. From a mechanistic perspective, the byproduct H_2O formed during RWGS competes with CO_2 and H_2 for active sites on catalyst surfaces, thereby inhibiting their adsorption efficiency and impeding the overall reaction progress[53]. Due to the inherent hydrophobicity of carbon-based materials, adsorbed H_2O molecules on their surfaces are significantly reduced, effectively alleviating this inhibition and enhancing overall RWGS performance[54].

Biomass templating enables the synthesis of carbon-based carriers that effectively improve the dispersion of metal nanoparticles on their surfaces. Azancot et al.[54] utilized cellulose as a biomass template to prepare Fe/cellulose-derived carbon (Fe/CDC) catalysts, achieving CO selectivity of 91.9% at 400 °C. Further modification with Mo to form Fe-Mo/CDC catalysts exhibited superior CO selectivity across all temperature ranges (Figure 5(a)). Tarifa et al.[53] applied nitrogen and boron co-doping strategy to modulate CDC carrier surface hydrophobicity. Experimental findings revealed that Fe-Mg/CDC catalysts with homogeneous dispersion of Fe and MgO nanoparticles exhibited high densities of basic active sites and exceptional metal-loading capabilities. Even under complex conditions with 20% water vapor content, this catalyst maintained a CO generation rate of 4.12 μmol/(min·m^2) (Figure 5(b)).

Porous carbon nitride (C_2N), a class of two-dimensional carbon-based materials, exhibits remarkable selectivity toward specific reactants owing to its distinctive nitrogen-doped configurations, thereby significantly enhancing target product selectivity through tailored catalytic pathways[55]. Gao et al.[55] employed DFT to elucidate the reaction mechanism of C_2N-supported catalysts in RWGS processes (Figure 6(a)). Their findings revealed that electron transfer between active metals and C_2N, coupled with directional surface aggregation of metal species, substantially amplifies catalytic efficiency. This enhancement is attributed to enhancing electronic activity at the interface, which lowers reaction activation energy and significantly facilitates low-temperature RWGS progression.

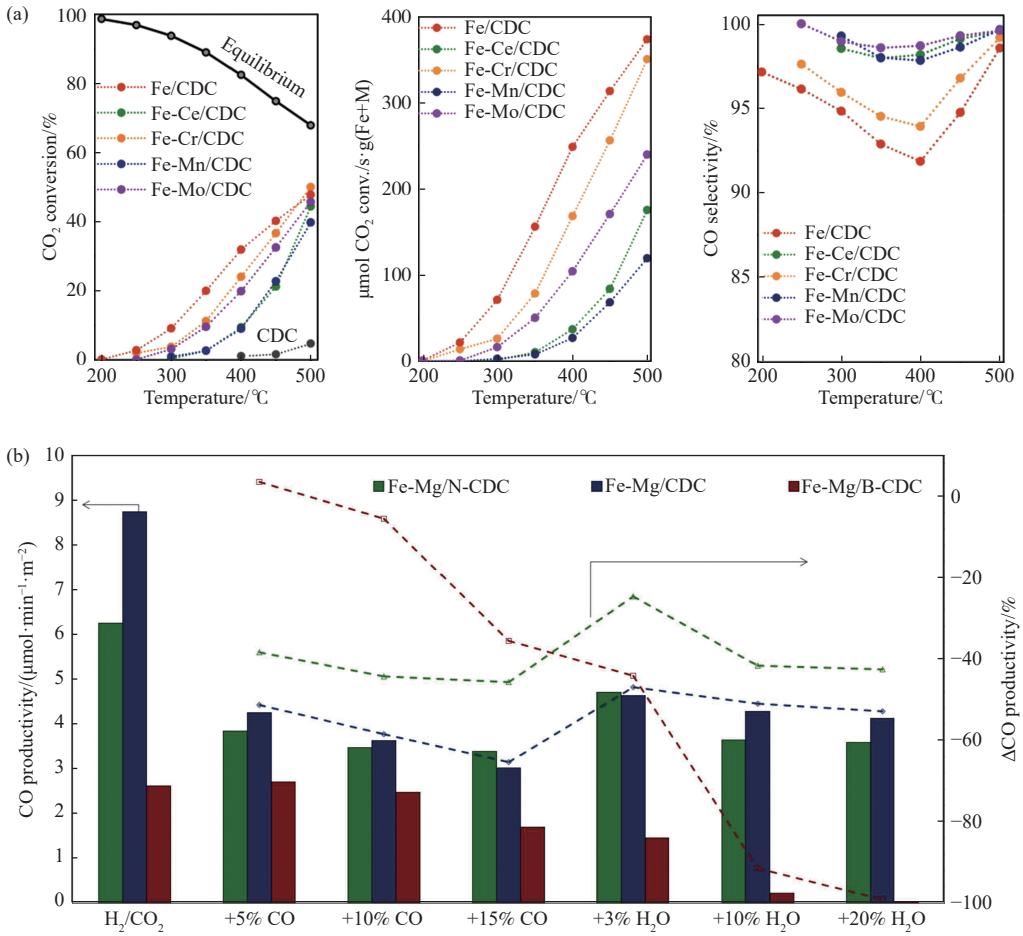


Fig. 5 (a) CO_2 conversion, airspeed and CO selectivity of the catalysts at 200−500 °C, (b) variation of catalytic activity with H_2/CO_2 feed[53−54]
(with permission from Elsevier)

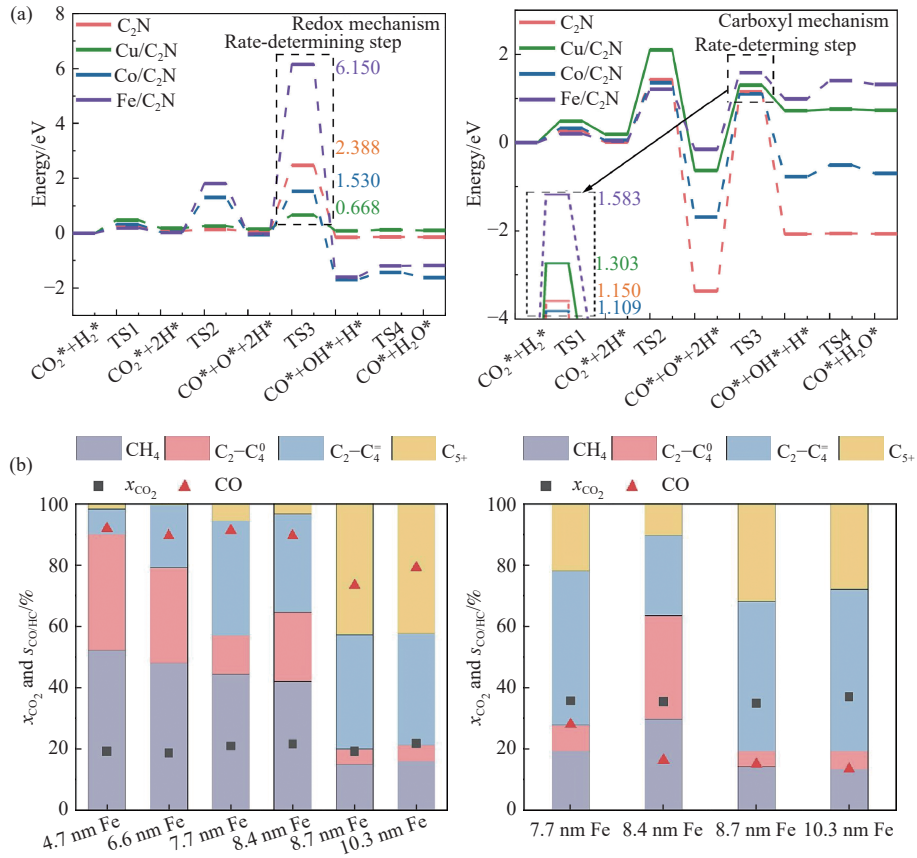


Fig. 6 (a) The energy barrier changes at each stage of the RWGS reaction catalyzed by C_2N and M/C_2N (M = Cu, Co, Fe) at low temperatures, redox and carboxylate mechanisms, (b) comparison of CO_2-FTS catalytic performance of catalysts with different particle sizes at CO_2 selectivities of 20% and 35%[55−56]
(with permission from Elsevier)

Parallel investigations demonstrated that at 20% CO_2 conversion by utilizing iron-based catalysts with potassium-modified carbon supports, and the near-90% CO selectivity observed across all four catalysts which feature iron particles with the size of 4.7−8.4 nm (Figure 6(b)) unequivocally confirmed the nanoparticle dimensions is pivotal in governing reaction selectivity[56].

In RWGS processes, H_2O as a byproduct competes with CO_2 for active sites, while the hydrophobic nature of carbon materials inherently mitigates this competition, conferring a distinctive edge over metal oxide carriers (a phenomenon where metal oxides may react with H_2O to form bicarbonates, impeding CO_2/H_2O diffusion and consequently limiting reaction kinetics[26]). In addition, strategic surface engineering, such as introducing fluorine functional group, can fortify H_2O resistance, rendering these materials favorable for humid industrial flue gas applications.

2.3 Carbon materials for dry reforming reaction

Methane dry reforming (DRM) technology offers a pathway to convert CH_4 and CO_2 into synthesis gas. Nevertheless, this process requires high temperature, typically exceeding 700 °C, which is detrimental to catalyst stability. Under such harsh environments, active components suffer from severe sintering, while carbon deposition accumulates on catalyst surfaces (as demonstrated in Equations (1)−(3)), thereby diminishing catalytic performance. Therefore, a fundamental conflict exists in DRM, where the high operating temperatures are necessary for the reaction but also accelerate catalyst degradation[57]. Carbon materials rich in defects, however, exhibit distinct structural advantages. Their intrinsic defect configurations enable precise modulation of electronic density surrounding the carbon skeleton, yielding dual benefits: enhanced electronic activity and significantly fortified adsorption/activation capabilities toward CO_2. These attributes collectively amplify molecular adsorption efficiency and elevate chemical conversion efficacy, making them promising candidates for mitigating the operational limitations encountered in traditional DRM processes[58].

$$CH_4 \rightleftarrows C + 2H_2 \quad \Delta H_{298K} = 74.9\ \text{kJ/mol} \qquad (1)$$

$$2CO \rightleftarrows C + CO_2 \quad \Delta H_{298K} = -173\ \text{kJ/mol} \qquad (2)$$

$$CO + H_2 \rightleftarrows C + H_2O \quad \Delta H_{298K} = -131.1\ \text{kJ/mol} \qquad (3)$$

Significant advancements have been achieved in modifying activated carbon-based catalysts for DRM applications. Through strategic N-doping, Sun et al.[59] developed activated carbons loaded with Co in conjunction

with Ce, Fe, or Zr elements. The study demonstrates that nitrogen incorporation effectively amplifies the Co^{2+}/Co^{3+} redox ratio while fortifying synergistic interactions between Co and Ce, a phenomenon that accelerates electron transfer kinetics. Moreover, nitrogen fortification enhances π-bond stability within the carbon support matrix, collectively boosting both catalytic activity and structural integrity (Figure 7(a)). In parallel investigations[60], Co-loaded activated carbon catalysts yielded exceptional performance under harsh 900 °C conditions: methane conversion rates reached 92% alongside CO_2 conversions of 98% (Figure 7(b)). The robust metal-support interactions that exist between Co and the activated carbon matrix are instrumental in preserving structural stability and sustained efficacy during prolonged reaction cycles.

In DRM applications, biochar-derived catalysts face significant challenges related to inadequate stability[61]. To address this limitation, Li et al.[62] engineered iron-enriched biochar catalysts by incorporating Fe_2O_3 into biomass precursors prior to pyrolysis. Remarkably, during a 160 min stability assessment, this catalyst exhibited only a 4.8% decline in methane conversion and a 3.1% reduction in CO_2 conversion. Such superior durability is primarily attributed to minimized *in situ* carbon consumption and minimal alterations in the pore structure. Alternatively, Zhang et al.[63] modified defect-rich biochar through Co and Ce co-doping. The investigation revealed that the defective biochar matrix provided anchoring sites for Co nanoparticles, effectively inhibiting their migration and agglomeration. Concurrently, elevated Co loading combined with enhanced dispersion generated additional active sites for DRM reactions. Furthermore, Ce incorporation could further optimize Co dispersity while expanding the quantity of active sites, thereby appreciably boosting the catalyst's overall activity (Figure 7(c)).

CNTs have emerged as ideal supports for DRM applications owing to their dual capability to anchor Ni/Co nanoparticles and suppress carbon deposition[58,64]. Ni-CNTs/mesoporous silica (MS) catalysts, synthesized by Donphai et al.[65] demonstrated exceptional thermal stability with stable H_2/CO ratios across temperature gradients of 650, 700 and 750 °C. This remarkable durability primarily stems from the inherent structural stability of CNTs, which collectively enhances catalytic activity and cyclic stability for dry reforming (Figure 8(a), (b)). In parallel research, Jiang et al.[58] engineered Co/N-CNTs catalysts achieving peak methane conversion of 92.9% and CO_2 conversion of 96.4%. Mechanistic elucidation revealed that carbon defect structures facilitate CH_4 activation, and nitrogen doping promotes Co-CNT interactions, ultimately increasing defect density and enhancing CO_2 adsorption capacity. These synergistic effects collectively drive efficient conversion of both reactants (Figure 8(c)). Alternatively, Wang et al.[64] developed a nickel-based CNT/CeO_2 nanocomposite designed as a microwave-responsive catalyst for microwave-assisted DRM processes. The relevant characterization indicated that optimized CNT architectures significantly enhance microwave absorption capabilities. Dielectric measurements demonstrated that high CNT content forms conductive networks, amplifying dielectric losses from the microwave electric field while intensifying magnetic losses induced by nickel nanoparticles. Leveraging this exceptional microwave responsiveness, the catalyst achieved CO_2 conversion of 90.1% and CH_4 conversion of 76.7% at ultralow microwave power (35 W, ~230 °C), maintaining stability beyond 50 h.

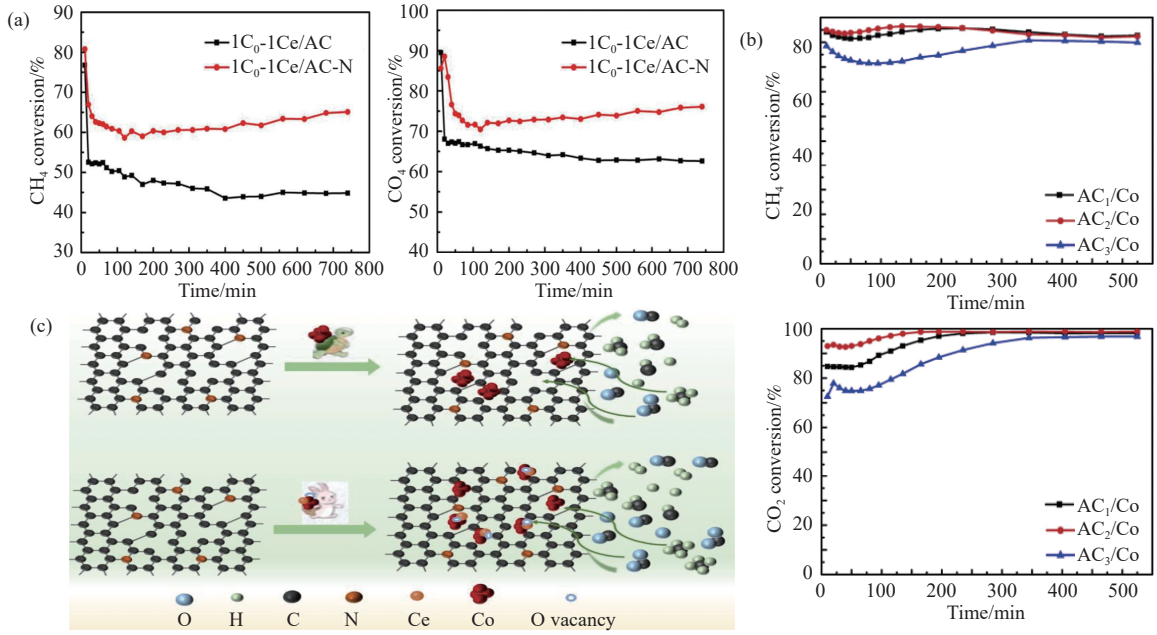


Fig. 7 (a) Durability test of catalysts for DRM at 800 ℃, (b) catalytic activity of various catalysts, (c) schematic illustration of the effect of Ce[59−60,63]
(with permission from Elsevier)

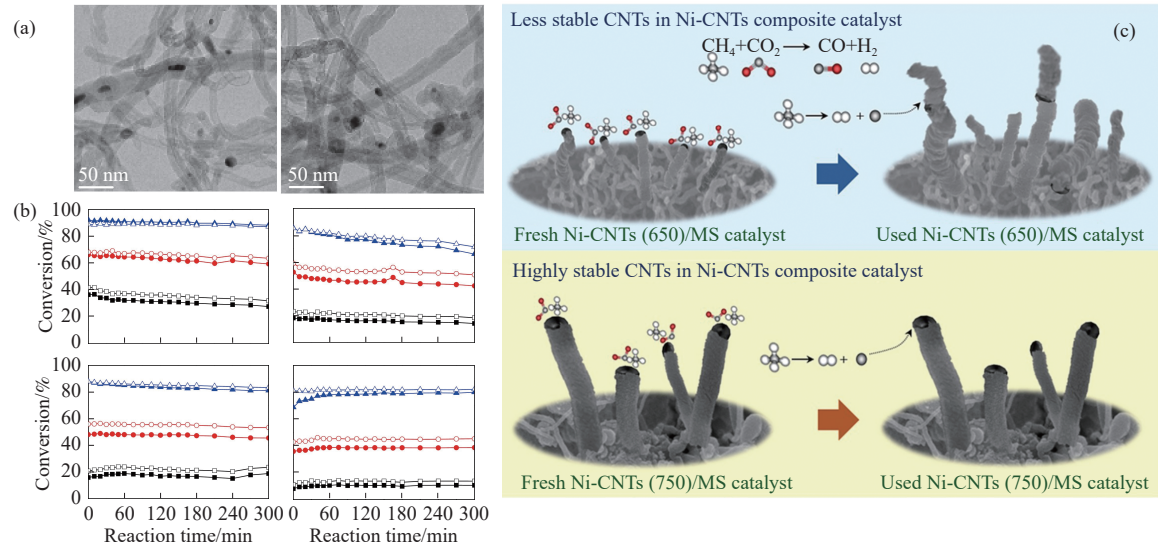


Fig. 8 (a) TEM images of Co/Ni-CNTs, (b) performance changes of Ni-CNTs/MS during DRM at different temperatures, (c) mechanism of methane-catalyzed CO_2 reforming reaction over Ni-CNTs/MS[58,65] (with permission from Elsevier)

2.4 Carbon materials for CO_2 hydrogenation to produce alcohols

Carbon-based supports have been extensively employed in catalytic hydrogenation of CO_2 to methanol[66–67]. However, in the more complex domain of CO_2 to ethanol synthesis, a process involving C−C coupling reactions, metal carbides have gained prominent application. This predominance stems from their exceptional ability to cleave C=O bond scission and facilitate C1 species chain growth[68].

CNTs exhibit pronounced advantages and synergistic effects in methanol synthesis. Dong et al.[66] engineered Cu-ZnO-Al_2O_3 hybrid catalysts supported by CNTs, and the catalysts demonstrates 44% enhancement in CO conversion and 25% increase in methanol yield compared to CNT-free counterparts. This superior performance primarily stems from CNTs' inherent hydrogen pre-reduction characteristics: within the 298−573 K temperature range, CNTs effectively adsorb and store molecular hydrogen. Concurrently, they establish a high-density hydrogenic microenvironment at catalyst surfaces, particularly near active sites, which substantially accelerates CO hydrogenation reaction kinetics. Notably, these CNT-enhanced catalysts lower the operating temperatures for methanol synthesis by 15−20 °C, thereby improving conversion efficiency and significantly boosting productivity. In complementary research, Din et al.[67] developed Cu/CNTs series catalysts featuring uniformly dispersed copper nanoparticles across CNT surfaces. Compared to traditional copper-supported systems, CNT carriers not only optimized spatial distribution of active sites but also substantially enhanced overall catalytic efficiency. The mechanistic role of CNT confinement effects on Pd-based catalysts for CO_2 hydrogenation was further elucidated by Wang et al.[69]. Results revealed that catalytic activity of Pd nanoparticles within CNTs was 3.7-fold higher than those external to tubes. This discrepancy originates from inhomogeneous distribution of $Pd^{\delta+}$ species, induced by radial density gradients, where interior sites possess higher $Pd^{\delta+}$ concentrations and greater stability. In the meanwhile, elevated H_2 partial pressure within CNT interiors further accelerated CO_2−H_2 reaction dynamics. Through theoretical simulations, Li et al.[70] investigated the potential of fluorinated-inner-surface CNTs (F_3-CNTs) in CO_2 reduction reactions (CO_2RR). Calculations demonstrated that F_3-CNTs possess high formation energy (−5.976 eV) and enhanced CO_2 adsorption capacity (19.043 eV). The catalytic pathway proceeds sequentially *via* RWGS and CO hydrogenation, ultimately yielding methanol as the primary product (Figure 9(a)). In methanol synthesis contexts, CNTs facilitate hydrogen adsorption and storage, while surface functionalization (e.g., methyl, thiol, or amino groups) further optimizes hydrogen adsorption-desorption cycling efficiency.

Carbide-supported active metal catalysts demonstrate exceptional catalytic proficiency in CO_2 hydrogenation toward ethanol synthesis. An efficient C−C coupling framework through Rh and K atom deposition onto β-Mo_2C supports were engineered by Ye et al.[68]. Within this reaction pathway, CO_2 is initially converted into methanol intermediates *via* Mo_2C catalysis, followed by Rh-propelled carbonylation to ultimately generate ethanol (Figure 9(b)). The incorporation of K effectively suppresses excessive H_2 activation, thereby enabling synergistic regulation of both CO_2 hydrogenation and C−C coupling reaction rates.

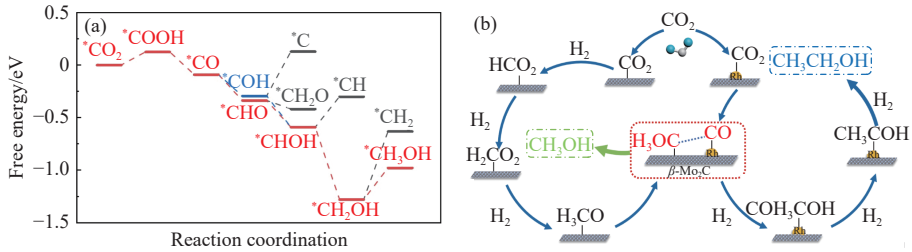


Fig. 9 (a) Free energy diagrams for the reduction of CO_2 to CH_3OH and the corresponding intermediates on F_3-CNTs, (b) catalytic mechanism of carbon dioxide hydrogenation to ethanol[68,70] (with permission from Elsevier)

2.5 Comparison of CO_2 catalytic performance between carbon-based and metal oxide-based materials

In CO_2 catalytic conversion, carbonaceous and metal oxide materials exhibit distinct characteristics, primarily differing in catalytic activity, product selectivity, and operational stability. Table 2 and Table 3 summarize the performance of carbon materials and metal oxides as carriers in the CO_2 methanation and dry reforming of methane reaction, respectively.

Table 2 Summary of the performance of metal oxides and carbon materials as methanation reaction carriers

Carrier type	Catalyst	Preparation method	Pyrolysis temperature /℃	Pressure (bar); Temperature /℃	BET surface area /($m^2 \cdot g^{-1}$)	Total pore volume /($cm^3 \cdot g^{-1}$)	n (H_2) /n (CO_2)	CO_2 conversion /%	CH_4 selectivity /%	Ref.
Metal oxides	2Ru-2Co/CeO_2	Ultrasonic-assisted co-impregnation	500	1; 450	2.40	0.00397	⩾ 4	69.97	84.84	[71]
	2Ru-2Mn/CeO_2	Ultrasonic-assisted co-impregnation	500	1; 450	3.02	0.00995	⩾ 4	67.03	90.31	[71]
	2Ni-2Co/CeO_2	Ultrasonic-assisted co-impregnation	500	1; 500	2.44	0.00424	⩾ 4	75.89	82.64	[71]
	12Ni/Al_2O_3	Ultrasonic-assisted co-impregnation	350	1; 350	137.4	0.38	4	30.2	86.4	[72]
	12Ni-4.5Ce/Al_2O_3	Ultrasonic-assisted co-impregnation	350	1; 350	125.1	0.34	4	64.5	97.5	[72]
	4Ru/Al_2O_3	Wetness incipient impregnation	500	375	172.0	0.382	4	85.0	98.0	[73]
Carbon-based	12Ni/CNTs	Ultrasonic-assisted co-impregnation	350	1; 350	196.7	0.38	4	61.1	96.6	[72]
	12Ni-4.5Ce/CNTs	Ultrasonic-assisted co-impregnation	350	1; 350	158.5	0.36	4	83.8	99.8	[72]
	15Ni/CNTs-N	Incipient wetness impregnation method	600	1; 400	225	0.44	4	81.2	99.2	[50]
	20Ni-5Ce/RGO	Modified Hummers method	400	1; 350	293.0	0.40	4	84.5	83.0	[46]
	15Ni/AC–N	Incipient wetness impregnation	600	1; 450	480.0	0.30	4	76.0	97.0	[43]
	Ni/Ce-ABC	Pyrolysis	600	1; 360	155.6	0.06	4	88.6	92.3	[45]
	0.5Ni/SCCB	Pyrolysis	500	1; 400	620.0	0.30	4	44	76	[44]
	Ru/N-ABC	Pyrolysis	480	1; 380	254	0.20	4	93.8	99.7	[74]

Table 3 Summary of the performance of metal oxides and carbon materials as reaction carriers for dry reforming of methane

Carrier type	Catalyst	Pressure (bar); Tem./℃	GHSV/ $(L\cdot(h\cdot g)^{-1})$	$n(CH_4)/n(CO_2)$	Time-on-stream/h	CO_2 conversion /%	CH_4 conversion /%	$n(H_2)/n(CO)$	Rate of carbon deposition	TOF	Ref.
Carbon-based	CMMW	1; 850	120	1	100	98	97	0.9−1.2	0.084 $g_c\cdot(g_{cat}\cdot h)^{-1}$	73.53 $mol\cdot(g_{cat}\cdot h)^{-1}$	[75]
	Ni/CNTs	1; 800	−	1	8	70.2	83.4	⩽ 1.0	0.093 $g_c\cdot(g_{cat}\cdot h)^{-1}$		[76]
	Ni-Co/SWCNTs	1; 900	−	1	72	−	−	−	No carbon deposition	230 $mol\cdot(g_{cat}\cdot h)^{-1}$	[77]
	Co/N-CNTs	1; 800	−	1	15	96.4	92.9	⩽ 1.0	−		[58]
	Ni-CNTs/MS	1; 550-750	24	1	5	0−90	10−100	< 1	−	1.25−10.35 s^{-1}	[65]
	Co-Ce/AC-N	1; 800	−	1	12.3	70−90	55−85		−	−	[59]
	Co/AC	1; 950	720	1	45	97.1	98.4	−	No carbon deposition	−	[78]
	Y-NC-Co	1; 850	14.4	1	24	86	75	0.8−1.0	−	−	[79]
	Fe-C	1; 800	2.4	0.5−2	2.7	95.2	90.8	0.92	−	−	[62]
Metal oxides	CoO_x–ThO_2	1; 850	20	0.91	15	93.7	84.8	−	0.2×10^3 $g_c\cdot(g_{cat}\cdot h)^{-1}$	124.1 $mol\cdot(g_{cat}\cdot h)^{-1}$	[80]
	CoO_x/MgO/silica–alumina	1; 850	20	0.91	7	93.9	99.0	−	0.16×10^3 $g_c\cdot(g_{cat}\cdot h)^{-1}$	174.2 $mol\cdot(g_{cat}\cdot h)^{-1}$	[80]
	CoO_x/ZrO_2/silica–alumina	1; 850	20	0.91	7	96.7	94.4	−	$< 0.1\times10^3$ $g_c\cdot(g_{cat}\cdot h)^{-1}$	166.1 $mol\cdot(g_{cat}\cdot h)^{-1}$	[80]
	Co/Al_2O_3	1; 700	36	1	−	~ 85	79.4	−	7.76%	−	[81]
	$Ni/MgAl_2O_3$	1; 750	−	1	4	81.7	95.3	0.73 ± 0.01	−	−	[82]
	Ni/Zr/MgO	1; 750	−	1	70	91	78	0.92	−	−	[83]
	Ni/ɤ-Al_2O_3-MgO	1	364	1	12	73	74.5	−	15%	−	[84]
	NiO/MgO/ZrO_2	1; 800	2516	1.5	−	100	54−97	1.1−2	31−33	−	[85]

The catalytic efficacy of carbonaceous substrates predominantly originates from their intrinsic defect-mediated electron transfer capabilities and surface defect architectures, whereas metal oxides rely on the chemical reactivity of metal-oxygen bonds to achieve CO_2 activation. Regulation mechanisms also diverge, carbonaceous materials leverage synergistic interplay between surface functional groups and porous architectures, while selectivity in metal oxides is impacted by the electronic configuration and oxidation states of metal cations. Furthermore, carbonaceous materials possess inherent advantages stemming from their chemical inertness and structural resilience; conversely, the stability of metal oxide systems is predominantly governed by lattice oxygen mobility and metal sintering phenomena.

3 Prospects for carbon materials in integrated CO_2 capture and utilization technologies

The ICCU technology presents an economically viable, high-efficiency approach that directly captures CO_2 from flue gas and *in situ* converts it into valuable chemical feedstocks, including CH_4, CO and H_2/CO syngas, thereby facilitating the production of high value chemical products[86]. In contrast to conventional CCU processes, ICCU eliminates the substantial energy requirements associated with intermediate cooling/heating, compression, and transportation steps, thereby streamlining reaction workflows and enhancing overall energy efficiency (Figure 10)[27]. Throughout this process, dual functional materials (DFMs) possessing both adsorptive and catalytic capabilities, play a key role in the CO_2 capture and *in situ* catalytic transformation cycle. While still in the nascent exploration stage, carbonaceous materials demonstrate significant potential for future development in ICCU system.

Carbonaceous materials typically exhibit high surface areas and porous architectures, facilitating the ultra-dispersion of active metal species. Their pronounced confinement effects enable the stabilization of metal nanoparticles at nanoscale dimensions, restricting migration and aggregation while concurrently modulating catalyst reducibility and activity[72].

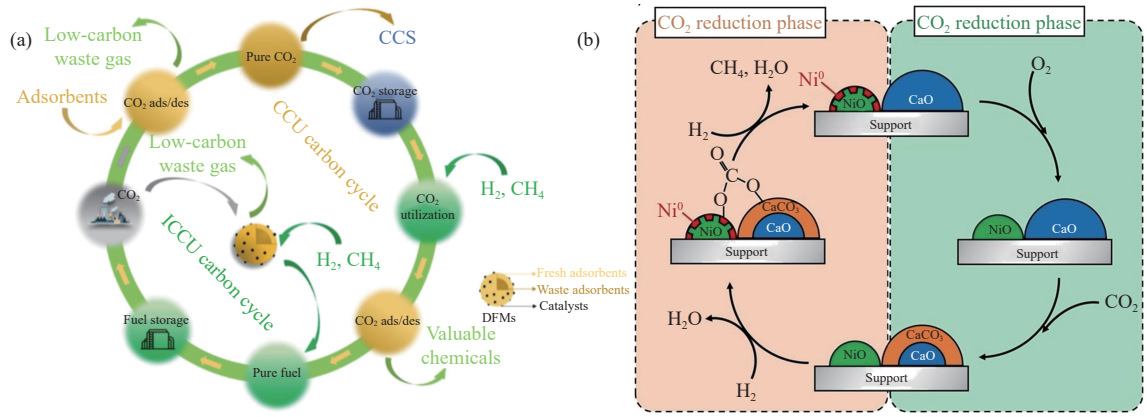


Fig. 10 (a) Schematic diagram of ICCU and its advantages over conventional CCU and CCS processes, (b) ICCU reaction mechanism[27]
(with permission from Elsevier)

Research by Guo[87] revealed that in Ni-based DFMs utilizing MWCNTs as supports, the weak metal-support interaction facilitates the reduction of NiO to highly metallic Ni, thereby enhancing methanation reaction kinetics and improving cyclic stability. Highly graphitized carbon materials, including CNTs, graphene, and analogous structures demonstrate outstanding electrical conductivity, which promotes electron transfer between reactants and active sites, thereby accelerating catalytic process[88]. Surface chemical modification can augment the basicity of carbonaceous materials, potentially extending the surface residence time of acidic CO_2 molecules and potentially elevating conversion rates[89]. When employed as modifiers, CNTs significantly enhance CO_2 sorption performance in metal oxides (e.g., CaO-based systems). For instance, the incorporation of 5% CNTs into $CaZrO_3$-CaO increases cumulative CO_2 capture by 53.57% after 15 cycles[23]. This finding suggests that introduction of carbonaceous materials may effectively strengthen the CO_2 capture capacity of DFMs, thus supplying additional carbon sources for subsequent conversion processes.

Although carbonaceous materials predominantly exhibit physical adsorption behavior at elevated temperatures and their modified functional groups are susceptible to thermal degradation, they manifest pronounced advantages when utilized as supports or modifying components. These materials excel in regulating metal dispersion, enhancing stability, and optimizing electron transport properties while simultaneously improving CO_2 adsorption capacity. Such multifaceted functionality unveils new avenues for developing highly efficient and stable DFMs for ICCU applications.

4 Conclusion and prospect

This work comprehensively reviews recent advancements in research concerning common carbonaceous materials, including activated carbon, porous carbon, graphene, and carbon nanotubes for CO_2 capture and utilization. Owing to their unique porous architectures and tailorable surface chemistry, these materials exhibit distinctive advantages in CO_2 adsorption. When employed as catalyst supports, the optimization of active sites *via* heteroatom doping or defect engineering can significantly enhance conversion efficiency toward high-value products such as CH_4, CO, H_2/CO syngas, and alcohols. Additionally, the application of carbon materials in the field of novel integrated CO_2 capture and conversion technologies is critically examined. Despite advances in CCU technologies employing carbonaceous materials, critical technical challenges persist for both carbonaceous adsorbents and carbon-based catalyst supports. Consequently, key challenges and future pathways are summarized as follows:

(1) Unmodified carbon materials primarily rely on van der Waals forces for physical adsorption, resulting in weak adsorption potential and significantly lower capacities than chemical adsorbents under low CO_2 concentration conditions. Loading metal oxide nanoparticles onto nitrogen-doped carbon surfaces can create dual-active sites, effectively reducing CO_2 adsorption energy and enhancing adsorption capacity. Traditional activated carbon suffers from low CO_2/N_2 selectivity, while nitrogen doping improves selectivity, the synergistic optimization of pore size modulation and basicity adjustment presents ongoing technical hurdles. Machine learning methods can elucidate intrinsic correlations between heteroatom doping concentrations, pore size distribution, and surface chemistry, providing theoretical foundations for precise control of functional groups and pore architectures. The development and large-scale application of high-performance materials such as graphene and CNTs are hindered by prohibitive production costs. Future efforts should prioritize low-cost, high-efficiency fabrication technologies, including continuous chemical vapor deposition processes and biomass-derived reductant synthesis to enable high-functional carbon materials to serve strategic carbon reduction and emission mitigation goals.

(2) The chemically inert nature of unfunctionalized carbon surfaces imposes high activation energy barriers for

CO_2 dissociation. Introducing heteroatoms can redistribute surface charge density, thereby weakening C=O bond strength. Although nitrogen doping enhances catalytic activity, the effect of distinct nitrogen configurations on product selectivity requires deeper mechanistic study. *In situ* spectroscopic techniques enable real-time observation of nitrogen speciation dynamics, facilitating more precise control over product distribution. Additionally, the design of bimetallic catalysts integrating synergistic catalytic properties of diverse metals can effectively modulate product distribution pathways, a strategy validated by recent studies.

With innovations in adsorption mechanism optimization, intelligent material design, cost-effective manufacturing, and precise control of catalytic active sites, carbon-based materials are primed to play increasingly pivotal roles in CO_2 capture and valorization. These advances offer novel directions for developing green, low-cost, and highly stable adsorbents and catalyst supports.

Declaration of Competing Interest

The authors declare no conflict of interest.

References

[1] FIRDAUS R M, DESFORGES A, RAHMAN MOHAMED A, et al. Progress in adsorption capacity of nanomaterials for carbon dioxide capture: A comparative study[J]. J Clean Prod, 2021, 328: 129553.

[2] DHILLON A, KUMAR D. Chapter 28 - New Generation Nano-Based Adsorbents for Water Purification[M]// THOMAS S, PASQUINI D, LEU S-Y, et al. Nanoscale Materials in Water Purification. Elsevier. 2019: 783−798.

[3] ZHANG Z, CANO Z P, LUO D, et al. Rational design of tailored porous carbon-based materials for CO_2 capture[J]. J Mater Chem A, 2019, 7(37): 20985−21003.

[4] DENG H, LI T, LI H, et al. Carbon-based adsorbents for CO_2 capture: A systematic review[J]. J Ind Eng Chem, 2025, 147: 39−55.

[5] LIU J, ZHONG X, CHEN G. Designing guidelines of coal-based porous carbon for CO_2 capture under flue gas conditions: A review[J]. Chem Eng J, 2025, 511: 162029.

[6] GOEL C, MOHAN S, DINESHA P. CO_2 capture by adsorption on biomass-derived activated char: A review[J]. Sci Total Environ, 2021, 798: 149296.

[7] DAS A, PEU S D, HOSSAIN M S, et al. Advancements in adsorption based carbon dioxide capture technologies- A comprehensive review[J]. Heliyon, 2023, 9(12): e22341.

[8] SUN J, LI H, LIU Q, et al. Recent advances in biomass-derived porous carbons for post-combustion CO_2 capture: From preparation and adsorption mechanisms to applications[J]. Chem Eng J, 2025, 520: 165890.

[9] WU W, WU C, LIU J, et al. Synergistic effects of heteroatom doping and narrow micropores on carbon dioxide capture in bamboo shoot shell-based porous carbon[J]. Sep Purif Technol, 2024, 339: 126690.

[10] GORBOUNOV M, DIAZ-VASSEUR E, DANACI D, et al. Chemical activation of porous carbon extracted from biomass combustion bottom ash for CO_2 adsorption[J]. Carbon Capture Sci Technol, 2024, 10: 100151.

[11] CHANG K Q, DONG Y H, LIAO K Y, et al. Waste foam to upcycled sponge-like porous carbon composites for efficient CO_2 capture and conversion[J]. J Environ Chem Eng, 2024, 12(3): 112565.

[12] YANG Y, LIU Y, LIU S, et al. Experimental and theoretical investigation of amine-modified biomass-derived activated carbon for CO_2 capture: The effects of carbon chain length and types of amine[J]. Chem Eng Sci, 2024, 292: 119968.

[13] WELDEKIDAN H, PATEL H, MOHANTY A, et al. Synthesis of porous and activated carbon from lemon peel waste for CO_2 adsorption[J]. Carbon Capture Sci Technol, 2024, 10: 100149.

[14] PHADUNGBUT P, KOO-AMORNPATTANA W, BUMROONGSRI P, et al. Adsorptive purification of CO_2/H_2 gas mixtures of spent disposable wooden chopstick-derived activated carbon: Optimal synthesis condition[J]. Sep Purif Technol, 2022, 291: 120948.

[15] SERAFIN J, DZIEJARSKI B, SREŃSCEK-NAZZAL J. An innovative and environmentally friendly bioorganic synthesis of activated carbon based on olive stones and its potential application for CO_2 capture[J]. Sustainable Mater Technol, 2023, 38: e00717.

[16] MALINI K, SELVAKUMAR D, KUMAR N S. Activated carbon from biomass: Preparation, factors improving basicity and surface properties for enhanced CO_2 capture capacity – A review[J]. J CO_2 Util, 2023, 67: 102318.

[17] GAO J, WANG H, LIU X, et al. Regulating CO_2 adsorption performance of lychee seed-based porous carbon materials: Insights into oxygen groups and pore structure[J]. Environ Res, 2025, 284: 122245.

[18] KUMAR JHA R, BHUNIA H, BASU S. UV activated monolithic graphene oxide-based adsorbents for dynamic CO_2 capture: Kinetic, isotherm and thermodynamic studies[J]. Chem Eng Sci, 2024, 285: 119572.

[19] ROBLE M, ZENSICH M, MORALES G M, et al. Chemical modification of graphene oxide for CO_2 capture: Impact on structure, defects, and adsorption behavior[J]. J Environ Chem Eng, 2025, 13(5): 118511.

[20] SAFAEI E, TALEBI Z, GHAFARINIA V. Optimizing the micro/mesoporous structure of hierarchical graphene aerogel for CO_2 capture by controlling the oxygen functional groups of graphene oxide[J]. J Taiwan Inst Chem Eng, 2025, 166: 105352.

[21] WU L, GUO R, CHANG G, et al. Interface engineering to regulate hollow one-dimensional N-doped Carbon@ZnO nanocomposite for boosting electromagnetic wave absorption[J]. Colloid Surf A-Physicochem Eng Asp, 2022, 654: 130156.

[22] OLIVEIRA H S, ARAÚJO L M, PINTO P C C, et al. Improvement on CO_2 capture by CaO pellet modified with carbon nanotubes[J]. Int Nano Lett, 2020, 10(2): 141−149.

[23] HEIDARI M, BORHAN MOUSAVI S, RAHMANI F, et al. The novel carbon nanotube-assisted development of highly

porous $CaZrO_3$-CaO xerogel with boosted sorption activity towards high-temperature cyclic CO_2 capture[J]. Energy Conv Manag, 2022, 274: 116461.

[24] IRANI M, JACOBSON A T, GASEM K A M, et al. Modified carbon nanotubes/tetraethylenepentamine for CO_2 capture[J]. Fuel, 2017, 206: 10−18.

[25] LEE M S, LEE S Y, PARK S J. Preparation and characterization of multi-walled carbon nanotubes impregnated with polyethyleneimine for carbon dioxide capture[J]. Int J Hydrog Energy, 2015, 40(8): 3415−3421.

[26] ZHAO C, CHEN X, ZHAO C. Carbonation behavior and the reaction kinetic of a new dry potassium-based sorbent for CO_2 capture[J]. Ind Eng Chem Res, 2012, 51(44): 14361−14366.

[27] SHEN Y, SUN S, SUN H, et al. Dual functional materials for integrated CO_2 capture and utilization (ICCU): Design, fabrication, performances, and challenges[J]. Chem Eng J, 2025, 512: 162440.

[28] CAM L M, HA N T T, KHU L V, et al. Carbon dioxide methanation over nickel catalysts supported on activated carbon at low temperature[J]. Aust J Chem, 2019, 72(12): 969−977.

[29] SUN F, LIU X, GAO J, et al. Highlighting the role of nitrogen doping in enhancing CO_2 uptake onto carbon surfaces: A combined experimental and computational analysis[J]. J Mater Chem A, 2016, 4(47): 18248−18252.

[30] LUO L, CHEN T, LI Z, et al. Heteroatom self-doped activated biocarbons from fir bark and their excellent performance for carbon dioxide adsorption[J]. J CO_2 Util, 2018, 25: 89−98.

[31] FUJIKI J, YOGO K. The increased CO_2 adsorption performance of chitosan-derived activated carbons with nitrogen-doping[J]. Chem Commun, 2016, 52(1): 186−189.

[32] CHOWDHURY S, BALASUBRAMANIAN R. Three-dimensional graphene-based porous adsorbents for postcombustion CO_2 capture[J]. Ind Eng Chem Res, 2016, 55(29): 7906−7916.

[33] HE X, LIU J, JIANG Y, et al. 'Useful' template synthesis of N-doped acicular hollow porous carbon/carbon-nanotubes for enhanced capture and selectivity of CO_2[J]. Chem Eng J, 2019, 361: 278−285.

[34] CHEN J, JIANG Y, LIU X, et al. One-step synthesis of CaO/CuO composite pellets for enhanced CO_2 capture performance in a combined Ca/Cu looping process *via* a facile gel-casting technique[J]. Sep Purif Technol, 2024, 328: 125057.

[35] ZHANG D, ZHANG Y, LEI P, et al. CaO-based adsorbents derived from municipal solid waste incineration bottom ash for CO_2 capture[J]. Sustainable Mater Technol, 2024, 39: e00856.

[36] SUN H, WANG Y, XU S, et al. Understanding the interaction between active sites and sorbents during the integrated carbon capture and utilization process[J]. Fuel, 2021, 286.

[37] CHAI K H, LEONG L K, SETHUPATHI S, et al. Carbon capture from low CO_2 concentration stream through ternary alkali metal nitrates promotion of MgO sorbents at intermediate temperature and low space velocity[J]. Chem Eng J Adv, 2024, 17: 100578.

[38] GUO Z K, GAO S, XIANG S X, et al. Mechanochemical synthesis of Ni/MgO dual functional materials at room temperature for CO_2 capture and methanation[J]. Chem Eng J, 2024, 481: 148599.

[39] CHEN Z, YAN X, HU X, et al. Amine-functionalized high-surface-area Al_2O_3 adsorbent for CO_2 capture: Effect of the support calcination conditions[J]. Sep Purif Technol, 2024, 342: 127064.

[40] SHEN X, YAN F, LI C, et al. Biogas upgrading *via* cyclic CO_2 adsorption: Application of highly regenerable PEI@nano-Al_2O_3 adsorbents with anti-urea properties[J]. Environ Sci Technol, 2021, 55(8): 5236−5247.

[41] FU H, SUN S, LIAN H. Enhanced low-temperature CO_2 methanation over Ni/ ZrO_2-Al_2O_3 catalyst: Effect of Al addition on catalytic performance and reaction mechanism[J]. J CO_2 Util, 2023, 69: 102415.

[42] QUATORZE I F, GONALVES L P L, KOLEN'KO Y V, et al. CO_2 methanation over Ni supported on carbon–ZrO_2: An optimization of the composite composition[J]. Catal Today, 2023, 422: 114215.

[43] GONALVES L P L, SOUSA J P S, SOARES O S G P, et al. The role of surface properties in CO_2 methanation over carbon-supported Ni catalysts and their promotion by Fe[J]. Catal Sci Technol, 2020, 10(21): 7217−7225.

[44] GAMAL A, TANG M, BHAKTA A K, et al. CO_2 methanation using sugarcane bagasse biochar/nickel sustainable catalysts[J]. Mater Today Sustainable, 2024, 25: 100627.

[45] WANG X, YANG M, ZHU X, et al. Experimental study and life cycle assessment of CO_2 methanation over biochar supported catalysts[J]. Appl Energy, 2020, 280: 115919.

[46] HU F, TONG S, LU K, et al. Reduced graphene oxide supported Ni-Ce catalysts for CO_2 methanation: The support and ceria promotion effects[J]. J CO_2 Util, 2019, 34: 676−687.

[47] ISAH M, LAWAL R, ONAIZI S A. CO_2 capture and conversion using graphene-based materials: A review on recent progresses and future outlooks[J]. Green Chem Eng, 2025, 6(3): 305−334.

[48] MA H, MA K, JI J, et al. Graphene intercalated Ni-SiO_2/GO-Ni-foam catalyst with enhanced reactivity and heat-transfer for CO_2 methanation[J]. Chem Eng Sci, 2019, 194: 10−21.

[49] MA M, ZHANG Y, GAO C, et al. Space confinement effect of carbon nanotube-alumina strip support on the Cu-Co catalysts for CO_2 methanation[J]. Catal Today, 2024, 437: 114781.

[50] GONALVES L P L, MELEDINA M, MELEDIN A, et al. Understanding the importance of N−doping for CNT-supported Ni catalysts for CO_2 methanation[J]. Carbon, 2022, 195: 35−43.

[51] MHADMHAN S, NGAMCHARUSSRIVICHAI C, HINCHIRANAN N, et al. Direct biogas upgrading *via* CO_2 methanation to high-quality biomethane over NiMg/CNT-SiO_2 fiber catalysts[J]. Fuel, 2022, 310: 122289.

[52] ZHAO CW, HUANG P, GUO Y. Advances and prospects of integrated carbon dioxide capture-hydrogenation conversion[J]. Clean Coal Technol, 2024, 30(4): 1−20.

[53] TARIFA P, GONZáLEZ-CASTAO M, CAZAA F, et al. Hydrophobic RWGS catalysts: Valorization of CO_2-rich streams in presence of CO/H_2O[J]. Catal Today, 2023, 423: 114276.

[54] AZANCOT L, TARIFA P, CAZAA F, et al. Fe-based catalysts on cellulose-derived carbon towards low-temperature RWGS[J]. Biomass Bioenergy, 2025, 199: 107894.

[55] GAO Z, MENG Y, SHEN H, et al. Theoretical study on low temperature reverse water gas shift (RWGS) mechanism on monatomic transition metal M doped C_2N catalyst (M=Cu, Co, Fe)[J]. Mol Catal, 2021, 516: 111992.

[56] MENG W, JONG B C A D, BOVENKAMP H V D, et al. Selectivity control between reverse water-gas shift and fischer-tropsch synthesis in carbon-supported iron-based catalysts for CO_2 hydrogenation[J]. Chem Eng J, 2024, 489: 151166.

[57] ZOU J, ZHAO L, HU Q, et al. Pyrolysis and catalytic reforming of disposable plastic waste for syngas production with adjustable H_2/CO ratio[J]. Appl Energy, 2024, 362: 122844.

[58] JIANG Z, SHI Y, BAI Y, et al. Pyridinic N and carbon defects synergistically promote methane dry reforming to syngas catalyzed by Co/N-CNTs[J]. Fuel, 2023, 337: 127136.

[59] SUN Y, ZHANG G, XU Y, et al. Comparative study on dry reforming of methane over Co-M (M = Ce, Fe, Zr) catalysts supported on N-doped activated carbon[J]. Fuel Process Technol, 2019, 192: 1−12.

[60] SUN Y, ZHANG G, LIU J, et al. Effect of different activated carbon support on CH_4-CO_2 reforming over Co-based catalysts[J]. Int J Hydrog Energy, 2018, 43(3): 1497−1507.

[61] CHEN Q M, LIU D W, L S M, et al. Research progress on the preparation process of biochar-based catalyst support for dry reforming of methane[J]. J Fuel Chem Technol, 2023, 51(3): 273−293.

[62] LI L, YAN K, CHEN J, et al. Fe-rich biomass derived char for microwave-assisted methane reforming with carbon dioxide[J]. Sci Total Environ, 2019, 657: 1357−1367.

[63] ZHANG X, LIU J, LI T, et al. Co-based defect-rich nanoarchitectonics with biomass carbon materials catalysts for CH_4–CO_2 reforming[J]. Mol Catal, 2023, 550: 113566.

[64] WANG T, LI X, LIU F, et al. Dielectrically optimized Ni/CeO_2/CNT catalysts for low-power and stable microwave-assisted dry reforming of methane[J]. Chem Eng J, 2025, 520: 166244.

[65] DONPHAI W, WITOON T, FAUNGNAWAKIJ K, et al. Carbon-structure affecting catalytic carbon dioxide reforming of methane reaction over Ni-carbon composites[J]. J CO_2 Util, 2016, 16: 245−256.

[66] DONG X, ZHANG H B, LIN G D, et al. Highly active CNT-promoted Cu-ZnO-Al_2O_3 catalyst for methanol synthesis from $H_2/CO/CO_2$[J]. Catal Lett, 2003, 85(3): 237−246.

[67] DIN I U, ALHARTHI A I, ALOTAIBI M A, et al. Deciphering the role of CNT for methanol fuel synthesis by CO_2 hydrogenation over Cu/CNT catalysts[J]. Chem Eng Res Des, 2023, 194: 115−120.

[68] YE X, MA J, YU W, et al. Construction of bifunctional single-atom catalysts on the optimized β-Mo_2C surface for highly selective hydrogenation of CO_2 into ethanol[J]. J Energy Chem, 2022, 67: 184−192.

[69] WANG J, LU S M, LI J, et al. A remarkable difference in CO_2 hydrogenation to methanol on Pd nanoparticles supported inside and outside of carbon nanotubes[J]. Chem Commun, 2015, 51(99): 17615−17618.

[70] LI Y, WANG L, ZHENG Z, et al. CO_2 thermoreduction to methanol on the F_3-CNT catalyst: A DFT study[J]. Surf Interfaces, 2025, 64: 106365.

[71] WASNIK C G, NAKAMURA M, SHIMADA T, et al. CO_2 methanation over low-loaded Ni-M, Ru-M (M = Co, Mn) catalysts supported on CeO_2 and SiC[J]. Carbon Resour Convers, 2025, 8(1): 100241.

[72] WANG W, CHU W, WANG N, et al. Mesoporous nickel catalyst supported on multi-walled carbon nanotubes for carbon dioxide methanation[J]. Int J Hydrog Energy, 2016, 41(2): 967−975.

[73] QUINDIMIL A, DE-LA-TORRE U, PEREDA-AYO B, et al. Effect of metal loading on the CO_2 methanation: A comparison between alumina supported Ni and Ru catalysts[J]. Catal Today, 2020, 356: 419−432.

[74] WANG X, LIU Y, ZHU L, et al. Biomass derived N-doped biochar as efficient catalyst supports for CO_2 methanation[J]. J CO_2 Util, 2019, 34: 733−741.

[75] KHAVARIAN M, CHAI S-P, MOHAMED A R. Direct use of as-synthesized multi-walled carbon nanotubes for carbon dioxide reforming of methane for producing synthesis gas[J]. Chem Eng J, 2014, 257: 200−208.

[76] MA Q, WANG D, WU M, et al. Effect of catalytic site position: Nickel nanocatalyst selectively loaded inside or outside carbon nanotubes for methane dry reforming[J]. Fuel, 2013, 108: 430−438.

[77] QU Y, SUTHERLAND A M, GUO T. Carbon dioxide reforming of methane by Ni/Co nanoparticle catalysts immobilized on single-walled carbon nanotubes[J]. Energy Fuels, 2008, 22(4): 2183−2187.

[78] ZHANG G, SU A, DU Y, et al. Catalytic performance of activated carbon supported cobalt catalyst for CO_2 reforming of CH_4[J]. J Colloid Interface Sci, 2014, 433: 149−155.

[79] ZHANG X, ZHANG G, LIU J, et al. Effects of defective structure originating from N incorporation-evaporation of Co-based biomass carbon catalysts on methane dry reforming[J]. Fuel, 2024, 357: 129752.

[80] MONDAL K C, CHOUDHARY V R, JOSHI U A. CO_2 reforming of methane to syngas over highly active and stable supported CoO_x (accompanied with MgO, ZrO_2 or CeO_2) catalysts[J]. Appl Catal A: Gen, 2007, 316(1): 47−52.

[81] CAO A N T, PHAM C Q, NGUYEN T M, et al. Dysprosium promotion on Co/Al_2O_3 catalysts towards enhanced hydrogen generation from methane dry reforming[J]. Fuel, 2022, 324: 124818.

[82] CHAUDHARY P K, KOSHTA N, DEO G. Effect of O_2 and temperature on the catalytic performance of Ni/Al_2O_3 and Ni/$MgAl_2O_4$ for the dry reforming of methane (DRM)[J]. Int J Hydrog Energy, 2020, 45(7): 4490−4500.

[83] CHATLA A, ALMANASSRA I W, KALLEM P, et al. Dry (CO_2) reforming of methane over zirconium promoted Ni-

MgO mixed oxide catalyst: Effect of Zr addition[J]. J CO_2 Util, 2022, 62: 102082.
[84] KHOJA A H, TAHIR M, AMIN N A S. Cold plasma dielectric barrier discharge reactor for dry reforming of methane over Ni/γ-Al_2O_3-MgO nanocomposite[J]. Fuel Process Technol, 2018, 178: 166−179.
[85] CHUENJAI M, WONGSAKULPHASATCH S, YONG N, et al. Synthesis of NiO/MgO/ZrO_2 catalyst for syngas production from partial oxidation and dry reforming of biogas[J]. Int J Hydrog Energy, 2022, 47(98): 41386−41396.
[86] GUO Z-L, BIAN X-L, DU Y-B, et al. Recent advances in integrated carbon dioxide capture and methanation technology[J]. J Fuel Chem Technol, 2023, 51(3): 293−302.
[87] GUO Z L. Experimental study on the integrated carbon dioxide capture and methanation process catalyzed by CaO-Ni materials[D]. Wuhan, China: Huazhong Agricultural University, 2023.
[88] BEHABTU N, YOUNG C C, TSENTALOVICH D E, et al. Strong, light, multifunctional fibers of carbon nanotubes with ultrahigh conductivity[J]. Science, 2013, 339(6116): 182−186.
[89] GONALVES L P L, MIELBY J, SOARES O S G P, et al. In situ investigation of the CO_2 methanation on carbon/ceria-supported Ni catalysts using modulation-excitation DRIFTS[J]. Appl Catal B: Environ, 2022, 312: 121376.

碳基材料应用于二氧化碳捕集与利用领域的研究进展

付　浪[1]，姚丁丁[1,*]，胡　强[2]，晏水平[1]，杨海平[2]

（1. 华中农业大学工学院, 湖北 武汉 430070; 2. 华中科技大学 煤燃烧国家重点实验室, 湖北 武汉 430074）

摘　要：CO_2 捕集与利用（CCU）技术作为应对全球气候变暖、推进碳减排及实现资源循环利用的关键技术，其核心材料的开发与性能优化备受关注。炭材料凭借可调孔隙结构、丰富表面活性位点、高比表面积及化学稳定性等独特物理化学性质，在 CO_2 捕集与利用领域展现出显著的应用潜力。本工作对活性炭、多孔碳、石墨烯以及碳纳米管等典型炭材料在碳捕集过程中的吸附行为特征及性能差异展开系统梳理；针对 CO_2 利用，对碳基材料在甲烷化、逆水煤气变换、甲烷干重整及醇类物质合成等典型 CCU 反应中的催化应用研究进展进行重点归纳；对炭材料在 CO_2 吸附容量、催化活性及稳定性等方面的优势与局限进行总结，并对其在集成 CO_2 捕集与利用一体化技术中的应用前景进行展望。对基于结构调控与表面改性碳质材料的关键策略进行提炼，以期为炭材料在今后 CCU 领域的研究和规模化应用提供理论参考。

关键词：CO_2 捕集与利用；炭材料；吸附；催化

中图分类号：X701　　**文献标识码：**A

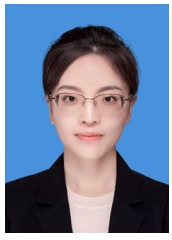
作者简介：



付浪（2001），硕士研究生，研究方向为碳基材料在二氧化碳捕集-甲烷化一体化技术中的应用研究，13114418890@163.com。



杨海平（1977），博士，华中科技大学教授，国家杰青、国家优青获得者。研究方向为含碳燃料热转化制备绿氢、液体燃料以及碳材料研究，yhping2002@163.com。



姚丁丁（1990），博士，副教授，研究方向为有机固废热解低碳高值转化，包含废塑料热解催化制碳纳米管、生物质催化气化制氢、碳捕集与转化，dingdingyao@mail.hzau.edu.cn。